Journal of the Chinese Institute of Engineers
Vol. 34, No. 1, January 2011, 11–17

Taylor & Francis
Taylor & Francis Group

The OSRM reaction over gold promoted copper zinc catalyst

Yuh-Jeen Huang*, Ke Lun Ng and Hsiao-Yu Huang

Department of Biomedical Engineering and Environmental Sciences, National Tsing Hua University, Hsinchu, Taiwan 30013, R.O.C.

(*Received 12 May 2010; final version received 12 June 2010*)

Hydrogen production by oxidative steam reforming of methanol (OSRM) was investigated over CuOZnO-based catalysts promoted by Au, which were prepared by using co-precipitation and deposition–precipitation and were characterized by X-ray powder diffraction (XRD), H_2-temperature programmed reduction (TPR), induced coupled plasma mass analyzer (ICP-MS), and transmission electron microscopy (TEM). We found that the reducibility of CuOZnO-based catalyst could be improved with increasing Au loading, which induced better performance at temperatures lower than 200°C. In addition, through calcination pretreatment, the residual chloride on the catalyst could be removed, which might expose more Au on the surface and result in a decrement of CO selectivity.

Keywords: OSRM; gold; promoter; CuOZnO-based catalyst; calcinations

1. Introduction

With increasing energy demand and ecological concerns, substitutions for fossil fuels have been under development for decades. Among all substitutes, the fuel cell system offers a high potential for power generation with few pollutants (Lindner and Sjomstrom 1984). The most promising fuel cells would seem to be the ones equipped with proton exchange membranes (PEM) in which hydrogen fuel is oxidized over a Pt electrode and electric energy is generated, with H_2O being the only reaction product. However, the distribution and on-board storage of hydrogen are major hurdles. In order to avoid using a high-pressure hydrogen tank, on-board fuel reforming to produce hydrogen for the fuel cell system is suggested. Methanol has been recommended as the best source of fuel for fuel cells among the high-energy density liquid fuels, due to the high H/C ratio, relatively low boiling point, easy storage and low risk of catalyst coking in the absence of C–C bonds (Bockris 1999).

There are several routes for hydrogen production from methanol, such as methanol decomposition (MD), steam reforming (SRM), partial oxidation (POM), and oxidative steam reforming (OSRM). The OSRM reaction is a combination of POM and SRM reactions. By tuning the ratios of methanol, oxygen, and steam, the reaction heat can be nearly neutralized. The OSRM reaction is a mild exothermic reaction and avoids hotspot formation; consequently, it reduces the risk of sintering (Pettersson *et al*. 2002). And, compared to the POM reaction, the OSRM reaction produces H_2 with lower CO levels.

Copper containing catalysts have been widely used in methanol synthesis, CO preferential oxidation, water gas shift reaction, and methanol reforming for hydrogen production (Atake *et al*. 2007, Marinõ *et al*. 2008, Rodriguez *et al*. 2009). Copper containing catalysts have the advantages of low cost, high selectivity, and activity. Turco *et al*. (2004a, 2004b) found that $Cu/ZnO/Al_2O_3$ exhibited significant activity during OSRM reactions at high temperatures, but at low temperatures (200–250°C) the dehydration and dehydrogenation dominated. Pant and Patel (2007) modified a copper zinc catalyst by introducing cerium and alumina. They found that a $Cu_{30}Zn_{20}Ce_{10}Al$ catalyst reached 100% methanol conversion at 280°C, but only 30% conversion when temperature decreased to 200°C. Most studies (Reitz *et al*. 2000, Turco *et al*. 2004b, Pant and Patel 2007) show that a high reaction temperature ($t > 250$°C) should be applied to get better catalytic performance. However, the PEMFC operating temperature is 80–180°C. To combine the reformer with PEMFC in one unit, high temperature will be a serious obstacle to overcome. In order to decrease the operating temperature without loss of catalytic activity, new materials will be needed.

*Corresponding author. Email: yjhuang@mx.nthu.edu.tw

ISSN 0253–3839 print/ISSN 2158–7299 online

DOI: 10.1080/02533839.2011.552962
http://www.informaworld.com

Gold, which is a very inactive element, has been regarded as a poor promoter of catalytic action. However, recent research has found that gold particles deposited on metal oxide by deposition precipitation or co-precipitation showed excellent catalysis promoting effect (Haruta 1997, Haruta and Daté 2001). Au deposited on ceria oxide, zinc oxide, aluminia oxide, and other metal oxides is found to promote great improvement in CO preferential oxidation (Nørskov *et al*. 2004). Au-doped catalysts are able to absorb CO at room temperature and oxidize it to CO_2 at mild temperatures (Haruta 1997). Manzoli *et al*. (2008) found that Au-promoted binary oxide, zinc oxide, and ceria oxide was the best combination for CO preferential oxidation. The CO conversion could reach 100% at 323 K, and even with the introduction of 10% steam, the conversion just slightly decreased by 0.01%.

Au nano particle added to several metal oxides for POM and DM reactions have been studied. Au deposited on different metal oxides for POM reactions was found to promote CO suppression and to promote catalytic ability (Chang *et al*. 2005, 2007, 2008, 2009 and Ou *et al*. 2008).

From literature reports, Au particles are excellent promoting agents in CO suppression and are able to function in methanol reforming. Meanwhile, compared to the SRM reaction, OSRM is able to operate at lower temperatures. Thus, the effect of Au added to copper zinc catalyst for OSRM reactions is of interest in this study. We hope that by the addition of Au, we can achieve a lower CO selectivity than a CuOZnO-based catalyst provides without losing catalytic performance in the OSRM reaction at low temperature.

2. Experimental

2.1. *Catalyst preparation*

$Au_{0.1}Cu_{30}ZnO$, $Au_{0.6}Cu_{30}ZnO$, and $Au_{2.5}Cu_{30}ZnO$ were prepared by co-precipitation method, and deposition precipitation. Copper nitrate and zinc nitrate were dissolved and mixed in deionized water at the concentration of 0.5 M. The samples were added, drop by drop, to 500 mL deionized water and vigorously stirred while 2 M Na_2CO_3 was added to maintain pH at 7. Meanwhile, an ultrasound probe, Microson X100, was immersed to provide sonication. 0.01 M of $HAuCl_4$ solution was dropped into the suspension of copper zinc nitrate mixed solution. The suspension was aged for 1 h after the addition of gold solution and the final suspension was then filtered and washed with 6 L deionized water. The final precipitant was purple blue color after it was dried at 105°C overnight. The catalysts were named $Au_xCu_{30}ZnO$-F as freshly prepared and $Au_xCu_{30}ZnO$-C400 after catalysts were calcined at 400°C with 30 mL min^{-1} air flow for 2 h.

2.2. *Catalyst characterization*

Inductively coupled plasma mass spectrometry (ICP-MS) was used for the determination of the metal content in each sample and the data are shown in Table 1. The measurements were performed with a Perkin Elmer SCIEX ELAN 5000, and the sample was dissolved in a mixture of HCl and HNO_3 acids before the measurements.

X-ray powder diffraction patterns were determined by Rigaku TTRAX III, equipped with 18 KW Rotating Anode Cu Target. The patterns were obtained from 20 degrees to 80 degrees at the rate of 4° per min.

Transmission electron microscopy was employed to observe the size and morphology of the catalysts. Catalyst powder was dispersed in absolute ethanol and sealed in the sample holder. After 30 min of sonication, a drop of the suspension was introduced onto a carbon-coated 200-mesh copper TEM grid. Imaging experiments were carried out on a JEOL JEM-2100 high-resolution transmission electron microscope, operating at 200 kV.

Temperature programmed reduction was carried out by following Yeh *et al*. (2009). In brief, a homemade temperature programmed reduction (TPR) system equipped with gold-coated TCD and Brooks 5850 E mass flow controller was employed for TPR test. 55 mg of sample was weighed and placed into a U-shaped quartz tube with 4 mm inner diameter. The samples were first purged by pure nitrogen for half an hour, followed by a 10% H_2/N_2 mixture with a flow of 30 mL min^{-1} for another half an hour. The TPR measurements were carried out from room temperature to 500°C at a rate of 7°C min^{-1} and the signal was connected to a computer and recorded.

2.3. *Catalytic activity measurement*

Figure 1 shows the schematic diagram of the system for the oxidation steam reforming of methanol. Catalytic activity measurements were carried out in a fixed-bed reactor operating at atmospheric pressure. The catalysts were pressed and sieved into 60–80 mesh and 100 mg of catalyst was placed into a 4 mm inner diameter quartz tube, stabilized by quartz wool at both ends. A thermal couple was in the center of the catalyst bed to control the reaction temperature. Liquid feed (H_2O/CH_3OH) and gaseous feed (O_2, Ar) were introduced by piston pumps and by Brooks 5850 E mass flow controller, respectively. The molar ratio of oxygen

Table 1. Chemical composition of $Au_xCu_{30}ZnO$ catalysts.

Name	Treatment after final precipitation	Composition (weight %)		
		Au	Cu	Zn
$Au_{0.1}Cu_{30}ZnO$-F	Dried at 105°C	0.09	30.4	69.5
$Au_{0.6}Cu_{30}ZnO$-F	Dried at 105°C	0.64	30.9	68.5
$Au_{2.5}Cu_{30}ZnO$-F	Dried at 105°C	2.45	31.1	66.5
$Cu_{30}ZnO$-F	Dried at 105°C	–	31	69
$Au_{0.1}Cu_{30}ZnO$-C400	Calcined at 400°C	0.08	30.4	69.5
$Au_{0.6}Cu_{30}ZnO$-C400	Calcined at 400°C	0.60	30.8	68.6
$Au_{2.5}Cu_{30}ZnO$-C400	Calcined at 400°C	2.47	31	66.5
$Cu_{30}ZnO$-C400	Calcined at 400°C	–	31	69

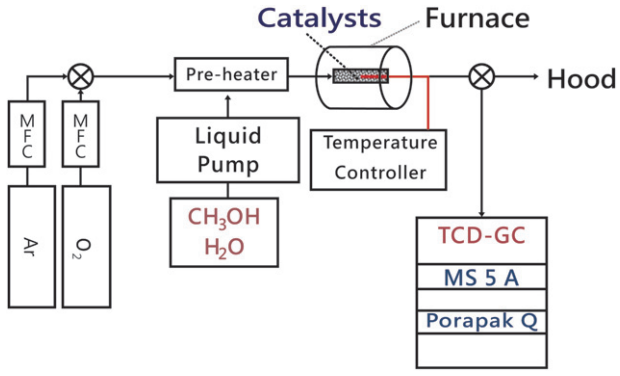

Figure 1. Schematic diagram of the system for the oxidation steam reforming of methanol.

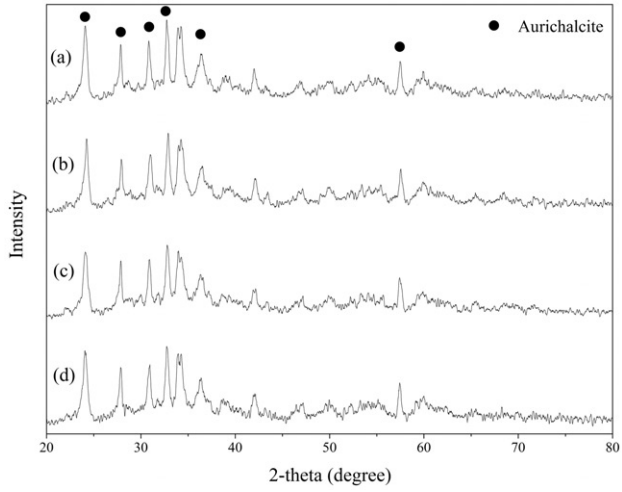

Figure 2. XRD patterns for non calcined catalysts: (a) $Au_{0.1}Cu_{30}ZnO$-F, (b) $Au_{0.6}Cu_{30}ZnO$-F, (c) $Au_{2.5}Cu_{30}ZnO$-F, and (d) $Cu_{30}ZnO$-F.

to methanol was 0.25 (O/M), and steam to methanol was 1.3 (W/M). Samples were collected in two sampling loops and sent to the gas chromatograph, China GC 2000, which was equipped with porapak Q and molecular sieve 5A columns and two TCD in parallel for the analysis of H_2, CO, CO_2, O_2, CH_4, CH_3OH, and H_2O.

The catalytic activation of the catalysts was evaluated in terms of their values of the conversion of MeOH (C_{MeOH}), selectivity toward CO formation (S_{CO}), to yield H_2 (Y_{H_2}). The C_{MeOH} was defined as the number of moles of reacted MeOH divided by the number of moles of MeOH added to the system. The S_{CO} was defined as the number of moles of CO produced divided by total number of moles of CO_2 and CO produced. The Y_{H_2} was defined as the rate of H_2 produced per unit catalyst.

3. Results and discussion

3.1. *XRD patterns*

The XRD pattern (Figure 2) showed that the fresh catalysts mostly existed in the aurichalcite ($Zn_3Cu_2(OH)_6(CO_3)_2$) form. However, after they were calcined by air at 400°C, all the aurichalcite reflection peaks were diminished and mainly decomposed to CuO and ZnO diffraction peaks (shown in Figure 3). Meantime, we also observed that the CuO diffraction peaks were weaker on the gold-loaded CuOZnO-based catalysts. It was assumed that the addition of gold might cause a reduction in CuO particle size. In addition, there were no gold diffraction peaks found in either calcined or non-calcined samples, showing that the gold particle size is too small to have long-range order.

3.2. *TEM*

The Au particles' sizes were estimated by transmission electron microscopy. The size before calcination was 3.2–4.6 nm and the size after calcination at 400°C for

2 h was 3.3–5.2 nm. Haruta (2004) indicated that nano gold particles which had a particle size larger than 2 nm were stable up to 670 K and this was also confirmed by our TEM image, as the Au particle size just increased a little bit after calcination. Meanwhile, because the atomic masses of Zn and Cu are very close, TEM is unable to distinguish whether these Au particles were deposited on the ZnO or CuO. But from the TEM image, we found that Au is highly dispersed over the surface areas, there was no selective deposition found.

Comparing Figure 4a with b, we found that the shape of Au particles remains spherical, even after calcination. But, on the copper–zinc-based catalyst, a shape change was observed, from pieces into meshes after calcination. The shape change should be due to the transformation of aurichalcite to CuO and ZnO.

3.3. *Temperature programmed reduction*

The temperature reductions of different gold loading catalysts with and without calcination are shown in Figure 5. We discovered that copper zinc samples without calcinations were composed of two main peaks, at 218°C and 244°C, respectively. The first peak was assumed to be the decomposition of the aurichalcite and the reduction of Cu^{2+} to Cu^{+} and the second peak would be the reduction of Cu^{+} to Cu^{0}. It is interesting that the samples promoted with Au were found to have another peak at 270°C. But with increasing gold loading, the peak shifted forward and combined with the peak at 260°C. These peaks were proposed as resulting from the residual chloride; in the absence of any $HAuCl_4$ precursor (Figure 5b), those peaks were not found.

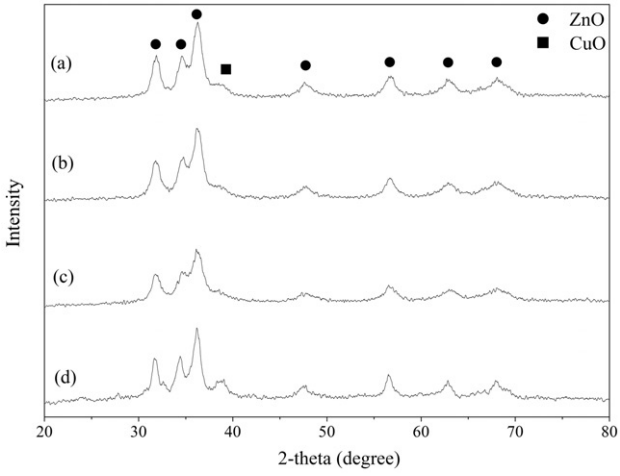

Figure 3. XRD patterns for calcined catalysts: (a) $Au_{0.1}Cu_{30}ZnO$-C400, (b) $Au_{0.6}Cu_{30}ZnO$-C400, (c) $Au_{2.5}Cu_{30}ZnO$-C400, and (d) $Cu_{30}ZnO$-C400.

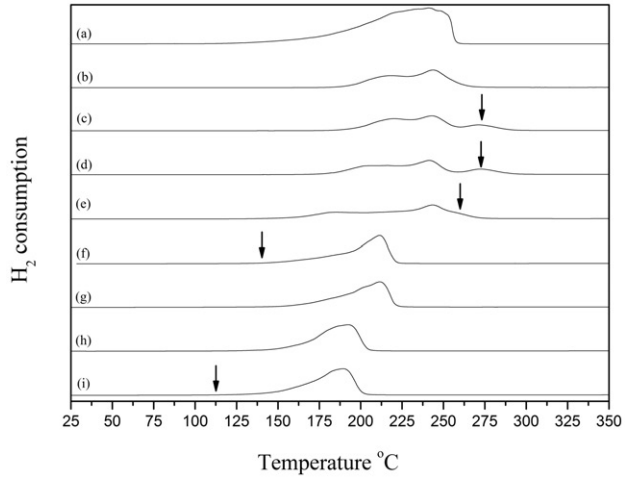

Figure 5. Hydrogen TPR profiles as hydrogen consumption versus temperature for calcined and non-calcined catalysts. (a) CuO, (b) $Cu_{30}ZnO$-F, (c) $Au_{0.1}Cu_{30}ZnO$-F, (d) $Au_{0.6}Cu_{30}ZnO$-F, (e) $Au_{2.5}Cu_{30}ZnO$-F, (f) $Cu_{30}ZnO$-C400, (g) $Au_{0.1}Cu_{30}ZnO$-C400, (h) $Au_{0.6}Cu_{30}ZnO$-C400, and (i) $Au_{2.5}Cu_{30}ZnO$-C400.

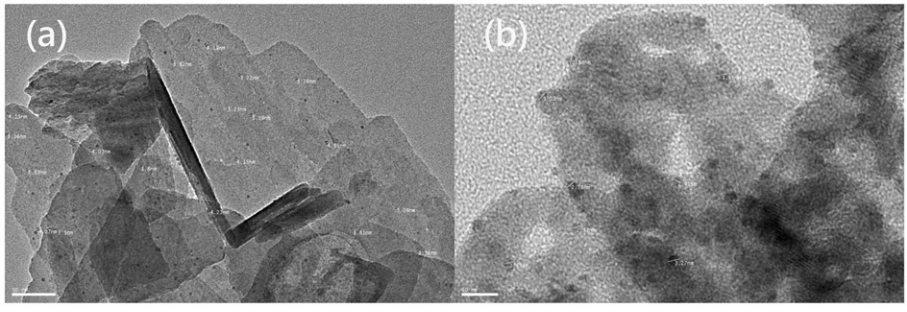

Figure 4. Transmission electron microscopy image of $Au_{2.5}Cu_{30}ZnO$ (a) before calcination and (b) after 2 h calcination.

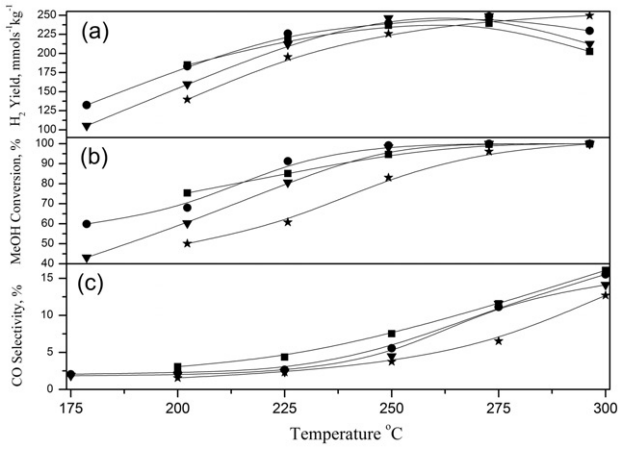

Figure 6. Temperature profiles of (a) hydrogen yield, (b) methanol conversion and (c) carbon monoxide selectivity for OSRM reaction over non calcined catalysts. O/M = 0.25, S/M = 1.3, GSHV = 60 K. (●) $Au_{0.1}Cu_{30}ZnO$-F, (▼) $Au_{0.6}Cu_{30}ZnO$-F, (☆) $Au_{2.5}Cu_{30}ZnO$-F, (■) $Cu_{30}ZnO$-F.

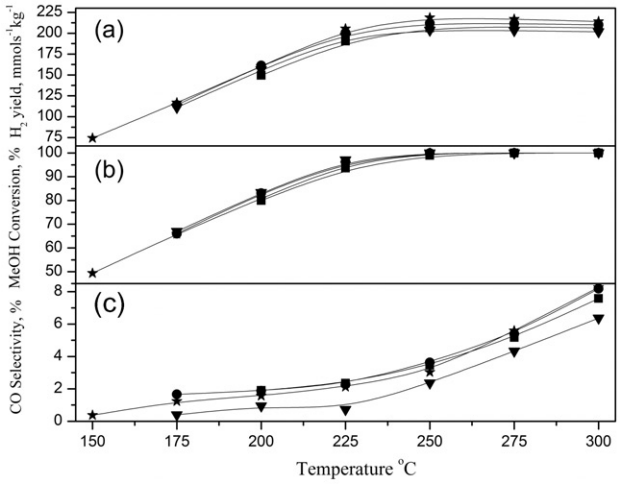

Figure 7. Temperature profiles of (a) hydrogen yield, (b) methanol conversion and (c) carbon monoxide selectivity for OSRM reaction over calcined catalyst. O/M = 0.25, S/M = 1.3, GSHV = 60 K. (●)$Au_{0.1}Cu_{30}ZnO$-C400, (▼) $Au_{0.6}Cu_{30}ZnO$-C400, (☆) $Au_{2.5}Cu_{30}ZnO$-C400, (■) $Cu_{30}ZnO$-C400.

The CuOZnO-based catalysts which were treated by calcination in air flow at 400°C showed a different reduction pattern. Only one peak with front shoulder was observed. For $Cu_{30}ZnO$ catalysts, the front shoulder, which was designated as the Cu^{2+} reduction to Cu^{+}, began from 150°C and merged with the main peak at 190°C. The main peak between 190°C and 215°C was assumed to be composed of two parts: (1) Cu^{+} reduced to Cu^{0}; (2) the isolated copper oxide directly reduced to metallic copper (Pettersson *et al.* 2002). Meanwhile, by increasing the load of Au, the reduction temperature will decrease, from 140°C (Figure 5f) to 110°C (Figure 5i). These phenomena showed that gold promoted the reducibility of catalysts at a lower temperature range. Besides, we discovered that with Au loading of more than 0.6%, the decrement of reduction temperature of the catalysts could reach 25°C. This demonstrated that the Au promoted CuO reduction at lower temperatures.

The third peak observed in the non-calcined samples was caused by the residual chloride which was not observed in the calcined samples. We concluded that calcination in air flow at high temperature could remove the residual chloride in the samples.

3.4. *Catalytic activity*

In order to find out the effect of calcination on the activity, the catalytic activity of non-calcined and calcined catalysts were compared. Figure 6 presents the catalytic activity of non-calcined catalysts in the OSRM reaction. Surprisingly, the data showed that all the CuOZnO-based catalysts with gold promoted had lower activity until test temperature was higher than 275°C. It is assumed that the residual chloride might seriously affect the catalytic ability at low temperature and result in worse catalytic performance than in non-promoted catalysts. After removing the chloride species at temperature >275°C (Figure 5c–e), the catalytic performance of catalyst may increase. Meantime, the AuCuOZnO catalysts displayed lower carbon monoxide selectivity compared to CuOZnO-based catalysts, but the overall carbon monoxide product was still higher than expected.

Figure 7 shows that better catalytic performance was observed in the activities of catalysts which had the residual chloride removed through the calcination process, in Au-promoted catalysts. All AuCuOZnO catalysts displayed higher methanol conversion and hydrogen yield than the CuOZnO-based catalysts, which indicated that Au could promote the reforming process and increase the hydrogen production. Interestingly, when increasing the Au loading on the copper zinc catalyst from 0.1%, 0.6%, to 2.5%, the reaction temperature for at least 50% methanol conversion was decreased from 175°C to 150°C, while copper zinc catalysts could not initiate the OSRM reaction at $T < 200$°C. It is suggested that gold may maintain the catalytic activity of CuOZnO catalysts at low temperatures.

The carbon monoxide selectivity from Figure 7 shows no linear relationship with the Au loading. The 0.6% gold weight percentage exhibited better carbon

monoxide suppression, but 2.5% had no significant difference from a CuOZnO-based catalyst. The optimal percentage of Au in the catalyst will be investigated in further research.

However, after calcination of the catalyst, only half of the carbon monoxide selectivity was observed and hydrogen yield slightly decreased. This shows that the decrement of CO may not come from the water gas shift reaction. Otherwise, the hydrogen yield should increase in the meantime. Shan *et al.* (2004) suggested another source of CO coming from the following reaction:

$$CH_3OH_{(g)} + 0.25O_2(g) \rightarrow 2H_{2(g)} + 0.5CO_{2(g)} + 0.5CO_{(g)} \quad (1)$$

Equation (1) shows a reaction which produces CO without altering hydrogen production. Therefore, Equation (1) was considered as a better explanation for non-calcined catalysts as a result of higher CO selectivity. We believe the residual chloride on the catalyst could be removed by the calcination procedure, which might expose more Au promoter on the surface and result in a decrease of CO selectivity.

However, the role of Au in the OSRM reaction is still not clear. We believe that gold particles could catalyze a reforming reaction and promote the reaction occurring on copper nearby at the same time. Further investigation on mechanisms is required to unravel the role of gold particles in the reforming reaction.

4. Conclusions

This study shows that CuOZnO-based catalysts promoted with Au, during OSRM reactions, could achieve better catalytic activity and CO suppression at low temperatures at the same time. The success of operating the reaction at a temperature lower than 180°C and the lower CO yield are significant results. They show the feasibility of the combination of PEMFC and methanol reforming in one unit for miniaturization and cost saving. However, catalytic performance at low temperature is still not commercially applicable. In further investigations, attempts to increase hydrogen yield should be emphasized.

Acknowledgments

The authors would like to thank the National Science Council (NSC) of the ROC for the financial support of this study under contract no. NSC-98-2221-E-007-029-MY3.

References

Atake, I., *et al.*, 2007. Production of hydrogen from methanol over Cu/ZnO and Cu/ZnO/Al_2O_3 catalysts prepared by homogeneous precipitation: steam reforming and oxidative steam reforming. *Journal of molecular catalysis A: chemical*, 275 (1–2), 130–138.

Bockris, J., 1999. Hydrogen Economy in the Future. *International journal hydrogen energy*, 24 (12), 1–15.

Chang, F.W., *et al.*, 2005. Production of hydrogen via partial oxidation of methanol over Au/TiO_2 catalysts. *Applied catalysis A: general*, 290 (1–2), 138–147.

Chang, F.W., *et al.*, 2009. Production of hydrogen by partial oxidation of methanol over bimetallic Au–Cu/TiO_2-Fe_2O_3 catalysts. *Journal of molecular catalysis A: chemical*, 313 (1–2), 55–64.

Chang, F.W., Lai, S.C., and Roselin, L.S., 2008. Hydrogen production by partial oxidation of methanol over ZnO-promoted Au/Al_2O_3 catalysts. *Journal of molecular catalysis A: chemical*, 282 (1–2), 129–135.

Chang, F.W., Yang, H.C., and Roselin, L.S., 2007. Hydrogen production by partial oxidation of methanol over Au/CuO/ZnO catalysts. *Journal of molecular catalysis A: chemical*, 276 (1–2), 184–190.

Haruta, M., 1997. Size- and support-dependency in the catalysis of gold. *Catalysis today*, 36 (1), 153–166.

Haruta, M., 2004. Gold as a novel catalyst in the 21st century: preparation, working mechanism and applications. *Gold bulletin*, 37 (1–2), 27–36.

Haruta, M. and Daté, M., 2001. Advances in the catalysis of Au nanoparticles. *Applied catalysis A: general*, 222 (1–2), 427–437.

Lindner, B. and Sjomstrom, K., 1984. Operation of an internal-combustion engine – lean conditions with hydrogen produced in an onboard methanol reforming unit. *Fuel*, 63 (11), 1485–1490.

Manzoli, M., *et al.*, 2008. Preferential CO oxidation in H_2-rich gas mixtures over au/doped ceria catalysts. *Catalysis today*, 138 (3–4), 239–243.

Marinõ, F., *et al.*, 2008. CO preferential oxidation over CuO–CeO_2 catalysts synthesized by the urea thermal decomposition method. *Catalysis today*, 133–135, 735–742.

Nørskov, J.K., *et al.*, 2004. On the origin of the catalytic activity of gold nanoparticles for low-temperature CO oxidation. *Journal of catalysis*, 223 (1), 232–235.

Ou, T.C., Chang, F.W., and Roselin, L.S., 2008. Production of hydrogen via partial oxidation of methanol over bimetallic Au–Cu/TiO_2 catalysts. *Journal of molecular catalysis A: chemical*, 293 (1–2), 8–16.

Pant, K.K. and Patel, S., 2007. Hydrogen production by oxidative steam reforming of methanol using ceria promoted copper–alumina catalysts. *Fuel processing technology*, 88 (8), 825–832.

Pettersson, L.J., Lindström, B., and Menon, P.G., 2002. Activity and characterization of Cu/Zn, Cu/Cr and Cu/Zr

on γ-alumina for methanol reforming for fuel cell vehicles. *Applied catalysis A: general*, 234 (1–2), 111–125.

Rodriguez, J.A., *et al*., 2009. Water-gas shift activity of Cu surfaces and Cu nanoparticles supported on metal oxides. *Catalysis today*, 143 (1–2), 45–50.

Reitz, T.L., *et al*., 2000. Characterization of CuO/ZnO under oxidizing conditions for the oxidative methanol reforming reaction. *Journal of molecular catalysis A: chemical*, 162 (1–2), 275–285.

Shan, W., *et al*., 2004. Oxidative steam reforming of methanol on $Ce_{0.9}Cu_{0.1}O_y$ catalysts prepared by deposition–precipitation, coprecipitation, and complexation–combustion methods. *Journal of catalysis*, 228 (1), 206–217.

Turco, M., *et al*., 2004a. Production of hydrogen from oxidative steam reforming of methanol I. Preparation and characterization of $Cu/ZnO/Al_2O_3$ catalysts from a hydrotalcite-like LDH precursor. *Journal of catalysis*, 228 (1), 43–55.

Turco, M., *et al*., 2004b. Production of hydrogen from oxidative steam reforming of methanol II. Catalytic activity and reaction mechanism on $Cu/ZnO/Al_2O_3$ hydrotalcite-derived catalysts. *Journal of catalysis*, 228 (1), 56–65.

Yeh, C.T., *et al*., 2009. Selective production of hydrogen from partial oxidation of methanol over supported silver catalysts prepared by method of redox coprecipitation. *Catalysis today*, 148 (1–2), 124–129.